Applied Thermal Engineering 68 (2014) 80–91

Contents lists available at ScienceDirect

Applied Thermal Engineering

journal homepage: www.elsevier.com/locate/apthermeng

# A heat transfer numerical model for thermoelectric generator with cylindrical shell and straight fins under steady-state conditions

Minfeng Zhou*, Yongling He, Yanmin Chen

*School of Transportation Science and Engineering, Beihang University, Xueyuan Road 37th, Haidian District, Beijing 100191, China*

## HIGHLIGHTS

- Proposed a new structure of TEG with cylindrical shell and straight fins.
- Validating the numerical model with a finite elements model in ANSYS Workbench.
- The average contribution rate to the output power can be utilised to evaluate the influence level of the input parameters.
- Obtaining the relevant conclusions that can be as reference to the early stages of future TEG designing.

## ARTICLE INFO

*Article history:*
Received 16 December 2013
Accepted 9 April 2014
Available online 19 April 2014

*Keywords:*
Thermoelectric generator
Cylindrical shell and straight fins
Heat transfer numerical model
Designing optimization

## ABSTRACT

Based on summarizing the latest research of vehicle exhaust thermoelectric generator (TEG), this paper proposes a newly designed TEG with cylindrical shell and straight fins. A two-dimensional heat transfer numerical model using finite difference method is established under steady-state conditions. This model is used to predict the output performance of TEG in different simulation conditions. The average contribution rate to the output power $CR_{var}$ is given in this paper to evaluate the influence level of different input parameters. Simulation results show that increasing the inlet temperature and the inlet mass flow rate of the exhaust, as well as reducing the inlet temperature of the coolant are useful methods to improve the performance of TEG in a certain extent. The heat transfer numerical model presented in this paper can be also applied to the numerical simulations and the optimization work on early designing stages of other types of TEG.



## 1. Introduction

As a new form of waste heat recovery application, thermoelectric generator (TEG) can absorb heat when there exists temperature difference, and transfer the heat directly into electricity, with the properties of no pollution, no noise, no moving parts, high reliability, long life, etc. This technology can be used in medical, military, energy industry, space technology and other fields [1,2]. Vehicle engine, as a typical representative of power machinery, has the conversion efficiency of fuel combustion only about 40%, and about 30%–45% of the total energy is taken away by engine exhaust. When a TEG is installed on the vehicle exhaust tube, the waste heat can be recovered and converted into electrical energy, which is stored in the vehicle battery or other energy storage devices for vehicle electronics equipment, improving the fuel economy of vehicles. Studies conducted by Stobart and Milner [3] have shown that based on the assumption of no increase in mass, a current market price of approximately $1000 would see the investment break even over the lifetime of the vehicle when a TEG device is utilised.

Although TEG has broad application prospects, due to the relatively low thermal conversion efficiency, it is still only at the stage of theoretical research and experimental demonstration without large-scale practical applications. The conversion efficiency of TEG can be improved from the following two aspects: increasing the thermoelectric material optimal value of ZT, as well as increasing the temperature difference between the hot and the cold sides of thermoelectric module (TEM) [4]. On the one hand, since the optimal value of ZT is an inherent property of thermoelectric material, improving the structure of thermoelectric material itself as much as possible can raise ZT value. But ZT values of large-scale commercial thermoelectric materials are generally not high, for example, this value of $Bi_2Te_3$ is only about 1. On the other hand, if conditions permit, efforts can be made on the optimization of TEG

* Corresponding author. Tel.: +86 13426015463.
*E-mail address:* zhouminfeng@ae.buaa.edu.cn (M. Zhou).

http://dx.doi.org/10.1016/j.applthermaleng.2014.04.018
1359-4311/

heat exchanger structure, such as improving the thermal environment to reduce heat loss, making the contact surface as flat as possible to reduce the thermal contact resistance, reducing the impact of intermediate links, etc. Increasing the temperature difference across TEMs can also improve the conversion efficiency of TEG.

Recently, for the purpose of improving the output power and the conversion efficiency of TEG, researchers have conducted lots of work on the numerical analysis and optimization of TEG heat exchanger models. Esarte et al. [5] made an analysis of the influence of fluid flow rate, heat exchanger geometry, fluid properties and inlet temperatures on the power supplied by TEG, these results can give those who have to design TEG a good idea about which operating conditions best meet the specifications required for a particular application. Suzuki and Tanaka [6,7] designed two types of geometric structure for TEG, multi-panels and cylindrical multi-tubes. The two structure types were both exposed to two thermal fluids directly, and the electric power generated by TEG was estimated respectively. The output power of the proposed 15 systems for multi-panels were deduced from heat transfer theory, and 6 systems for cylindrical multi-tubes were also investigated in that way of work. The results showed that each type of structure had the maximum power output in the case of ideal isothermal systems, and in the other realistic systems, there existed a certain system that supplied the maximum power output. Meng et al. [8] studied the complete model of a TEG with finned heat exchanger, taking into account the thermal irreversible effects. Through the simulation, it showed that TEMs can obtain 0.13 W output power and 0.87% the maximum conversion efficiency, it had also pointed out that the modelling method can effectively be applied to the low-quality heat recovery TEGs. Crane and Jackson [9] investigated thermoelectric waste heat recovery for current thermoelectric materials with advanced heat exchangers. A numerical model for heat exchanger integrated with thermoelectric models were created and validated against experimental data. It showed that the heat exchangers can achieve power densities over 40 W/l. Wang et al. [10] presented a mathematical model of a TEG device using the exhaust gas of vehicles as heat source. The model simulated the influence of the relevant factors on the output power and efficiency, such as exhaust mass flow rate, temperature and mass flow rate of different types of cooling fluid, convection heat transfer coefficient, etc. Hsiao et al. [11] established a numerical model combined a TEM, a cooling system and a one-dimensional thermal resistance model, and applied this model on two different potential positions, the exhaust tube and the radiator, to examine the feasibility. The maximum power density produced by the TEG was 51.13 mW/cm$^2$ when the temperature difference is 290 °C. The results showed that TEM presented better performance on the exhaust tube than on the radiator.

Currently, TEGs that being installed on the vehicle exhaust tube mainly have the structure of flat panels. Fig. 1a and b [12,13] respectively show the single-layered panel and the multi-layered panel structure. The panel-structured heat exchangers have the main advantages of simple, stable and reliable, making the TEMs heated and cooled sufficiently, lower cost and so on. However, the panel-structured heat exchanger changes the shape of the exhaust tube, which has lower portion of the space under vehicle chassis, causing difficulties in installation and maintenance. When the geometry shape of the exhaust tube changes, exhaust back pressure will be affected to some extent, which leads to the influence of the engine operating conditions. These factors limit large scale application of the panel structured heat exchanger TEG.

Based on summarizing the advantages and disadvantages of conventional structures of TEG, this paper proposes a newly designed TEG with cylindrical shell and straight fins. Since the heat transfer process during the operation of TEG is complex, including the heat conduction among various components and the heat convection between fluids and solids, the heat transfer numerical models for heat exchanger and TEM are established separately, which can evaluate the performance of TEG effectively. The goals of the numerical simulations include the temperature changes of exhaust and coolant in the axial direction, the temperature distribution on the fins, and the variations of output power and conversion efficiency of TEG. The simulations also focus on the thickness of the insulation layer of TEG, the exhaust and the coolant inlet temperatures as well as the inlet mass flow rate, the TEM positioning and other external factors, which may affect the TEG output characteristics. All these simulations are completed under steady-state conditions. The numerical model simulation analyses can help the TEG designers making choices of the relevant parameters, and provide appropriate guidance to complete the designing optimization of TEG. It also lay a solid foundation for future TEG simulations under transient conditions of vehicle engine.

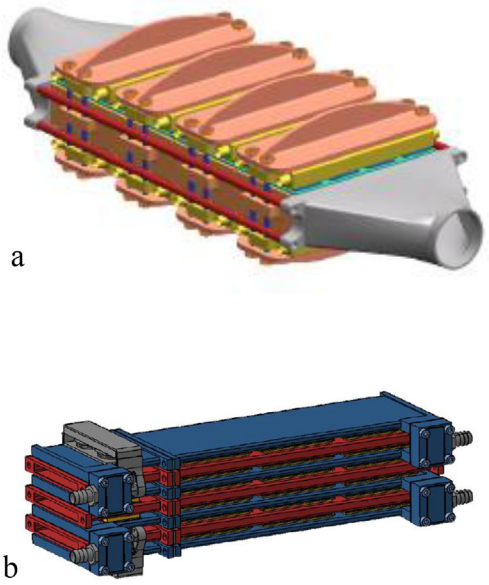


**Fig. 1.** a. TEG with single-layered panel heat exchanger. b. TEG with multi-layered panel heat exchanger.

## 2. Descriptions on the structure of TEG with cylindrical shell and straight fins

The conventional TEG which is on vehicle exhaust tube causes significant structural changes, insufficient contact of power generation devices, obvious influence on the engine exhaust back pressure, etc. To overcome these defects, this paper proposes a newly designed TEG with cylindrical shell and straight fins, whose schematic is shown in Fig. 2. This device is compact in structure and has high operational reliability, it can be also arranged on the position between the vehicle exhaust catalytic converter and the silencer to make the effective recovery of waste heat. Two semi-cylindrical shells directly contact the exhaust tube, which are joined as one unit by connecting bolts. Riveting fasten devices are used to support the heat transfer fins, TEMs and cooling tubes. The TEMs and heat transfer fins are in direct contact, avoiding the exhaust tube structural transformation, and it will not cause any influence on the engine exhaust back pressure. A certain number of symmetry fitting grooves on the semi-cylindrical shells are

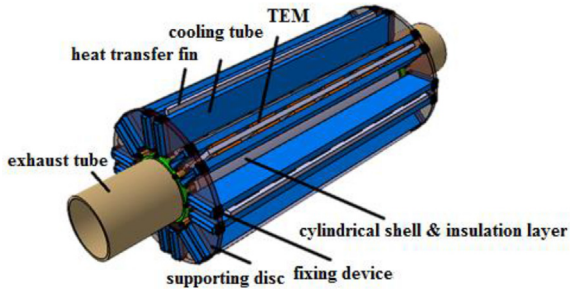


**Fig. 2.** Schematic of TEG with cylindrical shell and straight fins.

reserved, so the number of heat transfer fins can be changed optionally, accommodating the different power generation needs. The cooling tubes are branches of the engine cooling system, and the engine coolant flows into the tubes to cool down the cold sides of TEM. The cooling tubes are flat rectangular cross-section channels, which have unified specifications and convenient interfaces. Supporting discs with bolts connecting the semi-cylindrical shells are set on both ends of the cooling tubes, so that the whole TEG structure can be hold stably. This device has high thermal conversion efficiency, relatively low thermal resistance, and it can improve the exhaust waste heat recovery efficiency compared to those conventional vehicle exhaust TEG systems. It is also suitable for mass production and usage.

The semi-cylindrical shells that directly contact the exhaust tube are made of stainless steel, which is able to meet the needs of exhaust temperature for heat exchangers (the temperature of exhaust that is near the vehicle catalytic converter is about 500 °C). The heat transfer fins are made of aluminium alloy, which has good thermal performance and can maintain high enough temperature on the hot sides of TEM. A certain amount of thermal grease are smeared between the heat transfer fins and the hot sides of TEM, reducing the thermal contact resistance caused by the surface roughness in order to improve the thermal conductivity. The cooling tubes are also made of aluminium alloy. Due to the straight channel and thin-walled rectangular cross-section structure, they can directly be welded by using aluminium alloy sheets. The aluminium alloy cooling tubes are fixed on the TEG through two supporting discs with fastening devices at both ends. A certain preload is made, so the TEMs and the heat transfer fins can contact closely. Between the exhaust tube and the supporting discs, as well as the supporting discs and the connecting bolts of the semi-cylindrical shells, there exists some special washers, which are made of insulation material and can minimize the influence of the supporting discs heating effect on the coolant.

## 3. Heat transfer numerical model and validation

### 3.1. Numerical model description

From the schematic of TEG with cylindrical shell and straight fins which is shown in Fig. 2, it can be seen that the exhaust flows through the tube, so there exists heat convection between the exhaust and the tube wall. After being conducted through the tube wall and the cylindrical shell axially and radially, one part of heat flux flows to the heat transfer fins and the TEMs, while the other part is released into the surrounding environment by natural convection. The heat flux, which is conducted to the TEMs, is divided into two parts: one is transferred as electric power, and the other is conducted to the cold sides of TEM.

According to the general theory of numerical heat transfer, the first work to be carried out in modelling is the regional

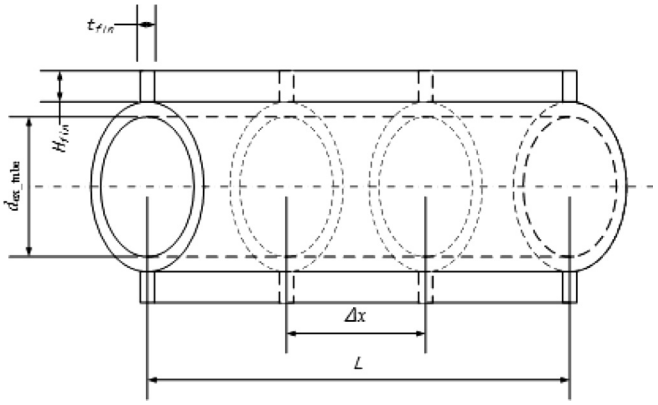


**Fig. 3.** Schematic of TEG model discretization in the axial direction.

discretization [14]. As it is shown in Fig. 3 (due to the symmetrical distribution of the heat transfer fins, there is only one pair of fins in the figure for simplification, the insulation layer and the cylindrical shell are also simplified to one layer), segmentation is made on the cylindrical shell, the TEMs and the cooling tubes in axial direction. The control volumes (CVs) are uniform in length, which is $\Delta x$ respectively, and $i$ represents the number of CV. Since TEG is central symmetry about the axis, conditions are all the same along the circumferential direction. The internal node method is used in grid generating process. The exhaust flow, exhaust tube wall, cylindrical shell, cooling tube wall and coolant are all in one-dimensional axial grid structure. To research the TEM output performance on different locations of the heat transfer fins, the thermocouples and the heat transfer fins involved in segment $i$ along the axial direction are divided into radial direction grids, whose lengths are $\Delta y$, so a two-dimensional grid structure is established on the heat transfer fins. The following assumptions are made to simplify the complex problem of modelling [1]:

i. The axial heat conduction within the thermocouples is ignored due to the dominion of the transverse conduction along the thermocouples.
ii. Thermal resistance through the exhaust tube wall, the cylindrical shell, the insulation layer, the ceramic plates, the metallic strips of TEMs and the cooling tube wall is taken into account as an equivalent thermal contact resistance.
iii. The radial length of the two-dimensional CV, $\Delta y$, is larger than the length of one single thermocouple, so the integrity of thermocouple can be ensured to complete the analysis.
iv. The gap between thermocouples is ignored.
v. Ignoring the radiation heat transfer and the heat losses between thermocouples and the heat transfer fins or the cooling tubes.
vi. The conducting heat flux between the insulation layer and the heat transfer fins is ignored.

Based on these assumptions, heat balance equations can be obtained for each CV of TEG numerical model.

The heat balance equation for exhaust flow is:

$$\begin{aligned}\dot{q}_{\mathrm{con\_ex},i} &= \dot{m}_{\mathrm{ex}} C_{\mathrm{ex}} \left(T_{\mathrm{ex},i} - T_{\mathrm{ex},i+1}\right) \\ &= h_{\mathrm{ex-wall}} \pi d_{\mathrm{ex\_tube}} \Delta x \left(T_{\mathrm{ex},i} - T_{\mathrm{tw},i}\right)\end{aligned} \quad (1)$$

The heat transfer coefficient between the exhaust flow and the exhaust tube wall $h_{\mathrm{ex\text{-}wall}}$ is given by the following equations [1]:

$$h_{\mathrm{ex-wall}} = Nu_{\mathrm{ex}} \lambda_{\mathrm{ex}} / d_{\mathrm{ex\_tube}} \quad (2)$$

$$Nu_f = \frac{\left(f_f/2\right)\left(Re_f - 1000\right)Pr_f}{1 + 2.7\left(f_f/2\right)^{1/2}\left(Pr_f^{2/3} - 1\right)} \tag{3}$$

$$f_f = A + \frac{B}{Re_f^{1/m}} \tag{4}$$

where for laminar flow ($Re_f < 2100$), $A = 0$, $B = 16.0$ and $m = 1.0$, for transition flow ($2100 < Re_f \le 4000$), $A = 0.0054$, $B = 2.3 \times 10^{-8}$ and $m = -0.6667$, and for turbulent flow ($Re_f > 4000$), $A = 0.00128$, $B = 0.1143$ and $m = 3.215$.

The exhaust tube wall, the cylindrical shell and the heat insulating layer can be viewed as three cylindrical layers (ignoring the volume of the insulation layer being spaced among the heat transfer fins), heat conduction process exists along the axial and the radial directions. The heat flux which is conducted from the internal layer along the radial direction can be thought as the total input heat flux to the external layer, so the following four sets of heat balance equations can be obtained.

The heat balance equations of the exhaust tube wall in each CV are:

$$\dot{q}_{con\_ex,i} = \dot{q}_{ex\_tube,radial} + \dot{q}_{ex\_tube,axial} \tag{5.1}$$

$$\dot{q}_{ex\_tube,radial} = \frac{T_{tw,i} - T_{cyl,i}}{\frac{1}{2\pi\lambda_{ex\_tube}\Delta x}\cdot\ln\left(1 + \frac{2t_{ex\_tube}}{d_{ex\_tube}}\right)} \tag{5.2}$$

$$\dot{q}_{ex\_tube,axial} = \frac{\pi\lambda_{ex\_tube}\left[\left(\frac{d_{ex\_tube}}{2} + t_{ex\_tube}\right)^2 - \left(\frac{d_{ex\_tube}}{2}\right)^2\right](2T_{tw,i} - T_{tw,i+1} - T_{tw,i-1})}{\Delta x} \tag{5.3}$$

The heat balance equations of the cylindrical shell in each CV are:

$$\dot{q}_{ex\_tube,radial} = \dot{q}_{cyl,radial} + \dot{q}_{cyl,axial} \tag{6.1}$$

$$\dot{q}_{cyl,radial} = \frac{T_{cyl,i} - T_{ins,i}}{\frac{1}{2\pi\lambda_{cyl}\Delta x}\cdot\ln\left(1 + \frac{2t_{cyl}}{d_{ex\_tube}+2t_{ex\_tube}}\right)} \tag{6.2}$$

$$\dot{q}_{cyl,axial} = \frac{\pi\lambda_{cyl}\left[\left(\frac{d_{ex\_tube}}{2} + t_{ex\_tube} + t_{cyl}\right)^2 - \left(\frac{d_{ex\_tube}}{2} + t_{ex\_tube}\right)^2\right]\left(2T_{cyl,i} - T_{cyl,i+1} - T_{cyl,i-1}\right)}{\Delta x} \tag{6.3}$$

The heat balance equations of the insulation layer in each CV are:

$$\dot{q}_{cyl,radial} = \dot{q}_{ins,radial} + \dot{q}_{ins,axial} + N_{fin}\dot{q}_{fin0} \tag{7.1}$$

$$\dot{q}_{ins,radial} = \frac{T_{ins,i} - T_{surf,i}}{\frac{1}{2\pi\lambda_{ins}\Delta x}\cdot\ln\left(1 + \frac{2t_{ins}}{d_{tube}+2t_{tube}+2t_{cyl}}\right)} \tag{7.2}$$

$$\dot{q}_{ins,axial} = \frac{\pi\lambda_{ins}\left[\left(\frac{d_{tube}}{2} + t_{tube} + t_{cyl} + t_{ins}\right)^2 - \left(\frac{d_{tube}}{2} + t_{tube} + t_{cyl}\right)^2\right](2T_{ins,i} - T_{ins,i+1} - T_{ins,i-1})}{\Delta x} \tag{7.3}$$

$\dot{q}_{fin0}$ is the heat flux being conducted to one of the heat transfer fins in each CV, $N_{fin}$ is the total number of the heat transfer fins.

The heat balance equations between the surface of insulation layer and the external environment in each CV are:

$$\dot{q}_{con\_ins} = h_{con\_air}\pi\left(d_{ex\_tube} + 2t_{ex\_tube} + 2t_{cyl} + 2t_{ins}\right) \times \Delta x\left(T_{surf,i} - T_{air}\right) \tag{8.1}$$

$$\dot{q}_{con\_ins} = \dot{q}_{ins,radial} \tag{8.2}$$

The natural air convection coefficient on the surface of the insulating layer $h_{con\_air}$ is [15]:

$$h_{con\_air} = Nu_{con\_air}\lambda_{air}\Big/\left(d_{ex\_tube} + 2t_{ex\_tube} + 2t_{cyl} + 2t_{ins}\right) \tag{9}$$

$$Nu_{con\_air} = C(Gr_{air}Pr_{air})^n = C(Ra)^n \tag{10}$$

For the horizontal cylinder, when $10^4 < Ra < 10^9$, $C = 0.53$, $n = 1/4$, when $10^9 < Ra < 10^{12}$, $C = 0.13$, $n = 1/3$.

$$Gr_{air} = \frac{\gamma g(T_{ins} - T_{air})\left(d_{tube} + 2t_{tube} + 2t_{cyl} + 2t_{ins}\right)^3}{\nu_{air}^2} \tag{11}$$

$$\gamma = \frac{2}{T_{ins} + T_{air}} \tag{12}$$

For the heat transfer fins, the schematic of discretization along the radial direction is shown in Fig. 4. Where, $b$ is the radial distance from the root of the heat transfer fin to TEM, $a$ is the side length of TEM.

Since the heat transfer fins are equipped with TEMs, the heat transfer conditions are not all the same for different positions. The thermal analyses of the fins should be divided into three parts. For $0 \le y < b$, there exists natural air convection on the surface of the heat transfer fin, the temperature distribution is in the presence of the second-order ordinary differential equation:

$$\frac{d^2T_{fin}}{dy^2} = \frac{2h_{fin\_air}}{\lambda_{fin}t_{fin}}\left(T_{fin} - T_{air}\right) \tag{13.1}$$

The central difference of second-order accuracy is used to transfer the ordinary differential equation into the following form:

$$\frac{T_{fin,i(k+1)} - 2T_{fin,ik} + T_{fin,i(k-1)}}{\Delta y^2} = \frac{2h_{fin\_air,ik}}{\lambda_{fin}t_{fin}}\left(T_{fin,ik} - T_{air}\right) \tag{13.2}$$

The initial conditions are:

$$\begin{aligned} T_{fin,i1} &= T_{ins,i}\lambda_{fin}\Delta x t_{fin}\frac{T_{fin,i2} - T_{fin,i1}}{\Delta y} \\ &= \dot{q}_{fin0} - 2h_{fin\_air,i1}\Delta x\Delta y\left(T_{fin,i1} - T_{air}\right) \end{aligned} \tag{14}$$

where the $h_{fin\_air,ik}$ is the $ik$th CV's two-dimensional natural convection coefficient. The total quantity of heat convection on one fin is (the upper and the lower side of the fin shown in Fig. 4 both has the same quantity of natural convention, and ignoring the area of two vertical sides since it is tiny):

$$\dot{q}_{air\_convection1} = 2\sum_{k=1}^{k_1} h_{fin\_air,ik}\Delta x\Delta y\left(T_{fin,ik} - T_{air}\right) \tag{15}$$

For $b < y \le a + b$, there exists the similar temperature distribution second ordinary differential equations:

$$\frac{d^2T_{fin}}{dy^2} = \frac{Q_h N_{TE}}{\lambda_{fin}t_{fin}LaN_{fin}} \tag{16.1}$$

$$\frac{T_{fin,i(k+1)} - 2T_{fin,ik} + T_{fin,i(k-1)}}{\Delta y^2} = \frac{Q_{h,ik}N_{TE}}{\lambda_{fin}t_{fin}LaN_{fin}} \tag{16.2}$$

In Eq. (16.2):

$$Q_{h,ik} = \alpha T_{th,ik}I + K\left(T_{th,ik} - T_{tc,ik}\right) - \frac{1}{2}I^2R \tag{17}$$

where $T_{th,ik}$ is equal to $T_{fin,ik}$, $R$ is the internal resistance of one thermocouple, which is the sum of the resistance of the thermocouple legs and the copper strip, that is:

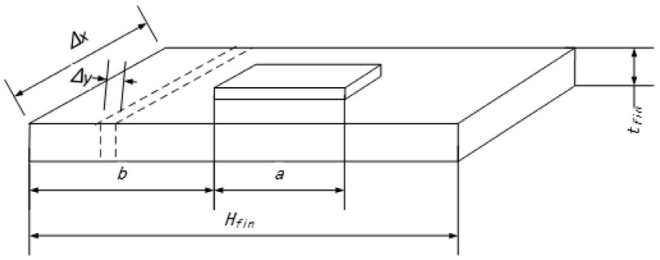


**Fig. 4.** Schematic of heat transfer fin model discretization in the radial direction.

$$R = 2\sigma L_{TEleg}\Big/A_{TEleg} + R_{copper} \tag{18}$$

where $L_{TEleg}$ and $A_{TEleg}$ are the length and the cross sectional area of the thermocouple leg respectively.

All the thermocouples are connected in series, so the current $I$ is determined by the number of thermocouples:

$$I = \frac{\sum_{i=1}^{n}\sum_{k=1}^{k_2}\alpha\left(T_{th,ik} - T_{tc,ik}\right)N_{fin}}{RN_{TE} + R_L} \tag{19}$$

$R_L$ is the total external resistance. The heat absorbed by the thermocouple in the whole CV is:

$$\dot{q}_{heat\_th,i} = \sum_{k=1}^{k_2} Q_{h,ik} \tag{20}$$

For $a + b < y \le H_{fin}$, the temperature distribution equation is the same with Eqs. (13.1) and (13.2), so the total quantity of heat convention between the fins and the air is:

$$\dot{q}_{air\_convection2} = 2\sum_{k=1}^{k_3} h_{fin\_air,ik}\Delta x\Delta y\left(T_{fin,ik} - T_{air}\right) \tag{21}$$

In Eqs. (15) and (19)–(21), $k_1$, $k_2$, $k_3$ refer to the different numbers of discrete units in each interval of $y$.

At last, the heat balance equation of a single fin in axial CV is:

$$\dot{q}_{fin0} = \dot{q}_{air\_convection1} + \dot{q}_{heat\_th,i} + \dot{q}_{air\_convection2} \tag{22}$$

In the CV shown in Fig. 3, the heat released from the cold side of TEM is:

$$\dot{q}_{heat\_tc,i} = \sum_{k=0}^{k_2} Q_{c,ik} \tag{23.1}$$

$$Q_{c,ik} = \left[\alpha T_{tc,ik}I + K\left(T_{th,ik} - T_{tc,ik}\right) + \frac{1}{2}I^2R\right]\frac{N_{TE}\Delta x\Delta y}{N_{fin}La} \tag{23.2}$$

The heat balance equations of the cooling tube wall in each CV are:

$$\dot{q}_{heat\_tc} = \dot{q}_{cw,radial} + \dot{q}_{cw,axial} \tag{24.1}$$

$$\dot{q}_{cw,radial} = \lambda_{ct}\Delta x w_{ct}\frac{T_{tc,i} - T_{ct,i}}{t_{ct}} \tag{24.2}$$

$$\dot{q}_{cw,axial} = \frac{\lambda_{ct}w_{ct}t_{ct}\left(2T_{ct,i} - T_{ct,i+1} - T_{ct,i-1}\right)}{\Delta x} \tag{24.3}$$

$T_{tc,i}$ is the mean value of $T_{tc,ik}$ on the whole discretization zone.

The heat balance equation between the coolant and the cooling tube wall is:

$$\begin{aligned} \dot{q}_{con\_cf,i} &= \dot{m}_{cf}C_{cf}\left(T_{cf,i} - T_{cf,i+1}\right) = h_{cf-wall}w_{ct}\Delta x\left(T_{ct,i} - T_{cf,i}\right) \\ &= \dot{q}_{cw,radial} \end{aligned} \tag{25}$$

The output power of TEG is:

$$P = \sum_{i=1}^{n} P_{\mathrm{i}} = \sum_{i=1}^{n} \left( \dot{q}_{\mathrm{heat\_th},i} - \dot{q}_{\mathrm{heat\_tc},i} \right) N_{\mathrm{fin}} \tag{26}$$

The TEM conversion efficiency is:

$$\eta_{\mathrm{TEM}} = \frac{P}{\sum_{i=1}^{n} \dot{q}_{\mathrm{heat\_th}} N_{\mathrm{fin}}} \tag{27}$$

and the TEG conversion efficiency of the whole numerical model is:

$$\eta_{\mathrm{TEG}} = \frac{P}{\sum_{i=1}^{n} \dot{q}_{\mathrm{con\_ex},i}} \tag{28}$$

### 3.2. Numerical process and validation

Along the axial direction, $\Delta x$, which is the length of each CV, ranges from 20 to 40 cm. Due to the mild temperature gradients across the exhaust tube, this level of discretization is adequate enough for the accurately modelling of the TEG numerical model across the full exhaust tube length. Because the radial dimensions of the fins are relatively small, the radial direction length of each CV $\Delta y$ varies from 0.4 to 1 cm. The solution methodology of this numerical model is implemented by using an iterative Newton–Raphson method. Since all the TEMs on one fin is connected electrically in series, the current $I$ is constant for all axial positions, which may influence the iteration speed of Newton–Raphson method, but it is still in a reasonable range.

In order to validate the accuracy of this numerical model, a finite elements model is built and analysed in ANSYS Workbench environment. The number of fins is 8, and all of the fins are symmetrical along the radial direction, so it is more practical and resource-saving to take one fin to simulate. One-eighth of the structure of this model is shown in Fig. 5. The boundary of the exhaust gas domain is added with the inflation layer to adapt the complex conditions on the interface between solid and fluid. There are 5 layers of the inflation and the total thickness is 1 cm. Other boundary conditions of this finite elements model, such as the natural convention between the outside surfaces of TEG components and air, the inlet and the outlet parameters of the exhaust and the cooling fluid, are consistent with the numerical model.

Figs. 6 and 7 show the output power and the heat conversion efficiency comparisons between the two models respectively under certain conditions when the exhaust inlet temperature changes. It can be observed that there are tiny discrepancies between the two models, mainly due to the intrinsic differences of the implementation of the two programs. The assumptions i and iv mentioned above could not be supported in ANSYS simulations, because the axial heat conduction of TEM and the gaps between them are taken into consideration in the program, which may influence the output performance of the ANSYS model. Besides, with the increasing number of CV, the calculation precision of the numerical model can be improved as well, leading to better consistence between these two models. Despite of these, the differences between the two models are within the allowable range, which validates that the proposed numerical model could be an equivalent thermal simulator to ANSYS in thermoelectric simulation.

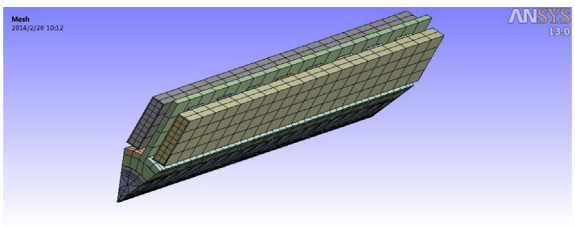


**Fig. 5.** Schematic of the finite elements model structure with grids (one-eighth).

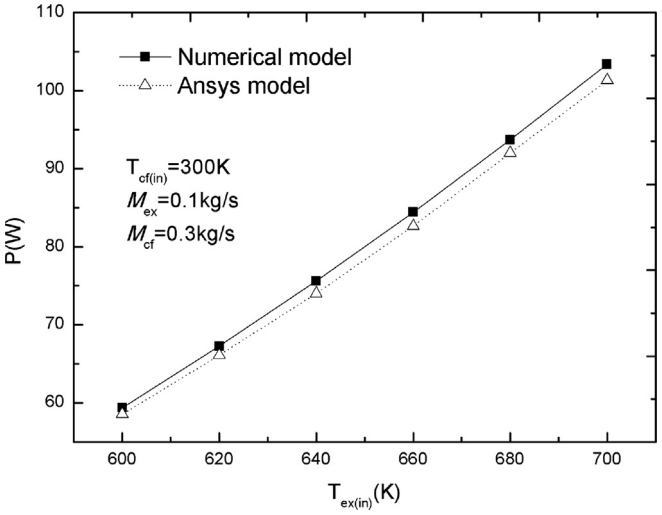


**Fig. 6.** Comparisons of the output power between the numerical model in Matlab and the finite elements model in ANSYS.

## 4. Simulation results and discussion

In the following numerical simulations, only under the steady state working conditions the TEG output performances are analysed. Transient working conditions analyses, which can study the output performances of TEG under the whole working cycle of engine, should be combined with a special engine simulation software, such as GT-POWER, for example, and this is not in the scope of this discussion.

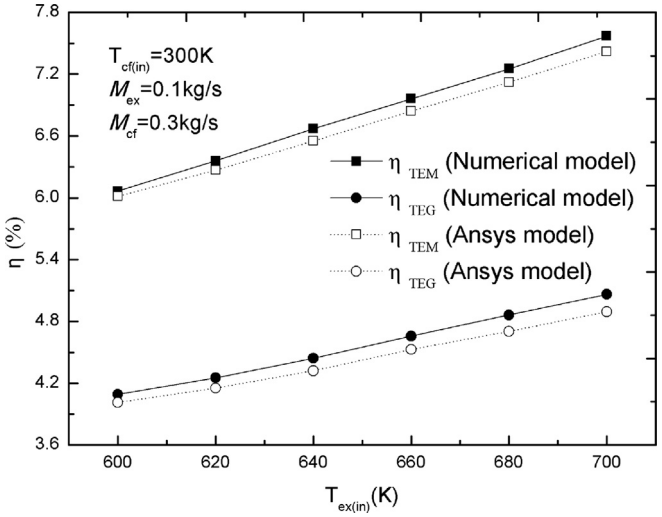


**Fig. 7.** Comparisons of the TEM and the TEG conversion efficiencies between the numerical model in Matlab and the finite elements model in ANSYS.

### 4.1. Parameter settings

Choosing a model with diesel engine exhaust tube size that matches the numerical simulation. The inner diameter of the exhaust tube is 60 mm, and the wall thickness is 3 mm. The length of the cylindrical shell is 685 mm, and the thickness is 10 mm. In order to ensure the heat losses as little as possible, and raise the temperature of the hot side of TEG, there sets an insulation layer outside the cylindrical shell. The radial height of the heat transfer fin is 60 mm, the thickness is 5 mm, and the length is equal to that of the cylindrical shell. The exhaust tube and the cylindrical shell are made of cast iron and nickel–chromium steel respectively, and the material of the insulation layer and the heat transfer fin are refractory slag wool and aluminium-silicon alloy respectively. The cooling tube is also made of aluminium-silicon alloy material, the cross-sectional dimensions are 34 mm × 10 mm, and the thickness is 1 mm.

As the engine exhaust temperature is relatively high, the semiconductor thermoelectric material in the middle temperature region (450–850 K) PbTe is used as the material of TEM, the dimension of each thermocouple is 1.5 mm × 1.5 mm × 2.0 mm, and the relevant physical parameters are $\alpha = 2.4 \times 10^{-4}$ V/K, $\lambda = 0.5$ W/(K m) , $\sigma = 1.2 \times 10^{-5}$ Ω m [16]. The P and N junctions of the thermocouples are connected by copper strips with the thickness of 0.3 mm. Between the copper strips and the heat transfer fins, as well as the copper strips and the cooling tubes, there exists some ceramic plates with the thicknesses of 0.7 mm. Although the thermal physical parameters of the material change with the temperature, in order to facilitate the numerical simulation, the temperature which is near the base of the heat transfer fins is selected as the reference temperature. In the entire simulation process, the physical parameters are set to be constant. The load resistance value is set to be equal to the total internal resistance of the thermocouples, so the maximum output power can be achieved under the same conditions [17]. Tables 1a and b show the relevant physical parameters in numerical simulation.

The inlet temperature of the exhaust flow is set to be 773 K (500 °C), and the flow velocity is 60 m/s. As the coolant in the TEG cooling system is supplied by the engine cooling system, the inlet temperature of the coolant is set to be 353 K (80 °C), and the flow velocity is 1 m/s. In different simulation conditions, the inlet temperature and the flow velocity of the exhaust and the coolant are recognized as the adjustable variables. The correlations mentioned above on the heat transfer coefficient in the numerical model can still be chosen because the Reynolds and Prandtl numbers are still within the extent of its validation. Exhaust and coolant flows are parallel flow type.

### 4.2. Simulation results

Fig. 8 shows the temperature variations of the exhaust and the coolant along the axial direction when the TEG model is axially divided into 20 average discrete CVs, the thickness of the insulation layer is 10 mm and $b$ is 15 mm. As it can be seen, the temperature of exhaust and the coolant are linear variations. Different from the conventional heat exchangers, due to the Seebeck effect, the TEM transforms part of the heat absorbed from the hot sides into electrical energy, resulting the heat released to the coolant is less than that absorbed from the hot sides of TEM. So the temperature distribution is linear, and this conclusion is consistent with the literature [1]. Unlike [1], which used water as both the hot and the cooling fluids to cause the similar temperature variation ranges, during the simulation process in this paper, the hot fluid is exhaust whose specific heat capacity and density are relatively small, while the cooling fluid is engine coolant whose specific heat capacity and density are relatively high, so the temperature variation range of the exhaust is larger than that of the coolant. Due to this limited coolant temperature variation range, there is not too much influence on the performance of TEG whether the exhaust and the coolant flow type is parallel or counter, and this will bring great convenience on practical applications of engineering.

Fig. 9 shows the temperature distributions along the radial direction for each CV on one fin (all the fins are radially symmetrical, so it takes one fin to represent all without considering the influence of convention caused by the gravity of air), the thickness of the insulation layer is 10 mm and $b$ is 15 mm, the natural convection heat transfer coefficient is assumed to be constant. As it can be seen, the temperature distributions of the fin are not linear, larger temperature drops happens near the base of the fin. In the middle part of the fin, which is also the place of the TEM hot sides being laid, heat flux is absorbed by TEM, so the temperature continues to drop. There is relatively little amount of heat being conducted to the last part of the fin, and it is all taken away to the environment through natural convection, the temperature drop is relatively slow. It is concluded that, since the severe temperature drop near the base of the fins, the arrangements of TEM should be as near to the base of the fins as possible. In other words, the smaller $b$ is, the higher temperature of the hot sides of TEM is. The related discussions will be given later in this section.

**Table 1a**
Relevant physical parameters of solids in the numerical simulation.

| | $\rho$ (kg/m$^3$) | $\lambda$ (W/(m K)) | $\sigma$ (Ω m) | $\alpha$ (V/K) |
|---|---|---|---|---|
| Exhaust tube | 7570 | 28.7 | – | – |
| Cylindrical shell | 7820 | 22.2 | – | – |
| Insulation layer | 350 | 0.067 | – | – |
| Heat transfer fin | 2660 | 180 | – | – |
| Thermocouple | 8200 | 0.5 | $1.2 \times 10^{-5}$ | $2.4 \times 10^{-4}$ |
| Copper strip | 8930 | 372 | $1.75 \times 10^{-8}$ | – |
| Ceramic plate | 3970 | 17 | $1.1 \times 10^{2}$ | – |
| Cooling tube | 2660 | 180 | – | – |

**Table 1b**
Relevant physical parameters of liquid and gases in the numerical simulation.

| | $\rho$ (kg/m$^3$) | $\lambda$ (W/(m K)) | $C_p$ (J/(kg K)) | $\mu$ (kg/(m s)) | $Pr$ |
|---|---|---|---|---|---|
| Exhaust flow (773 K) | 0.457 | 0.0656 | 1185 | $3.48 \times 10^{-5}$ | 0.63 |
| Coolant (353 K) | 971.8 | 0.674 | 4195 | $3.551 \times 10^{-4}$ | 2.21 |
| Air (300 K) | 1.165 | 0.0276 | 1005 | $1.86 \times 10^{-5}$ | 0.701 |

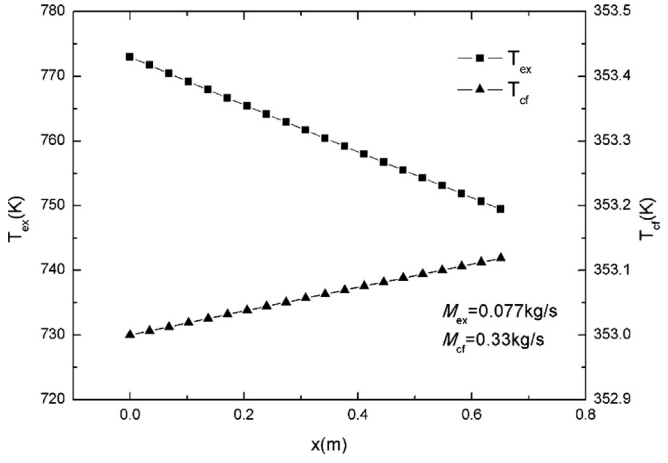


**Fig. 8.** Temperature variations of the exhaust and the coolant along the axial direction.

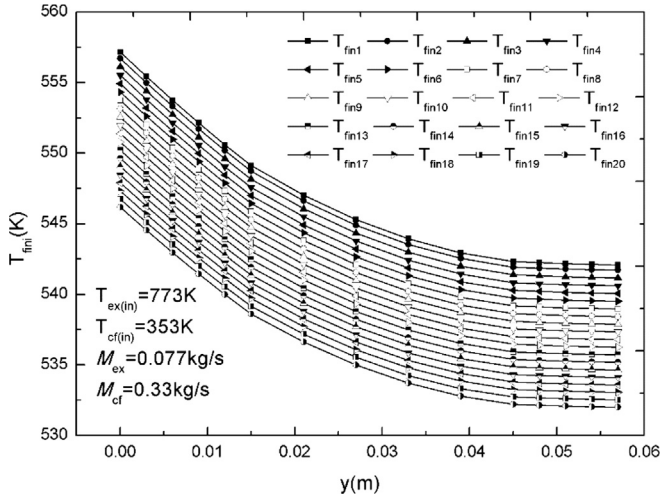


**Fig. 9.** Temperature distributions along the radial direction for each CV on one fin.

Fig. 10 shows the output power, the TEM conversion efficiency and the TEG conversion efficiency of each CV, the thickness of the insulation layer is 10 mm and $b$ is 15 mm. As it can be seen, with the axial temperature drop of the exhaust, the output power and the conversion efficiencies of each CV decrease linearly. The TEG conversion efficiency is less than the TEM conversion efficiency about 2%, which is caused by the heat losses through natural convection on the surface of the insulation layer and the heat transfer fins.

The following numerical analysis mainly focus on the adjustable variables of TEG. To evaluate the influence degree of each variable to the output performance of TEG, an evaluation index is defined as "the average variable contribution rate to the output power", $CR_{var}$, which is in the following form:

$$CR_{\mathrm{var}} = \frac{\sum_{m=1}^{j-1} \frac{P_{m+1}-P_m}{\mathrm{variable}_{m+1}-\mathrm{variable}_m}}{j-1} \tag{29}$$

where $j$ refers to the number of the sample points of the variable variation range, $P_m$ and $P_{m+1}$ refer to the output power of the whole TEG model at the adjacent sample points, meanwhile $\mathrm{variable}_m$ and $\mathrm{variable}_{m+1}$ refer to the corresponding value of variable at the adjacent sample points.

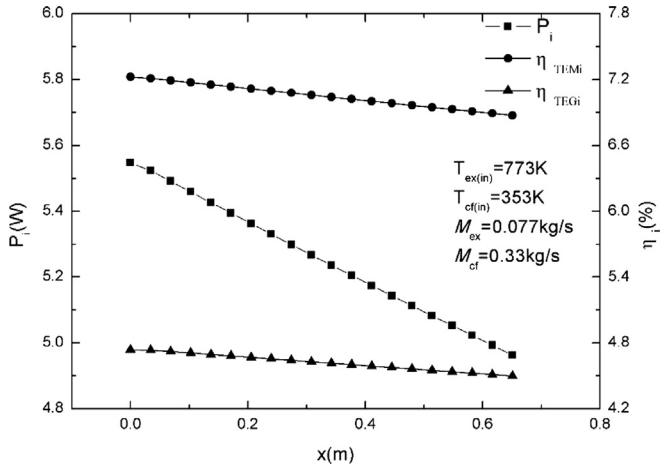


**Fig. 10.** Output power, TEM conversion efficiency and TEG conversion efficiency of each CV.

Firstly, assuming the material of insulation layer is unchanged, the output power, the TEM conversion efficiency and the TEG conversion efficiency of each CV are researched under the conditions that the thickness of insulation layer is 5 mm, 10 mm and 15 mm respectively, $b$ is 15 mm, as showed in Fig. 11a–c. It is seen

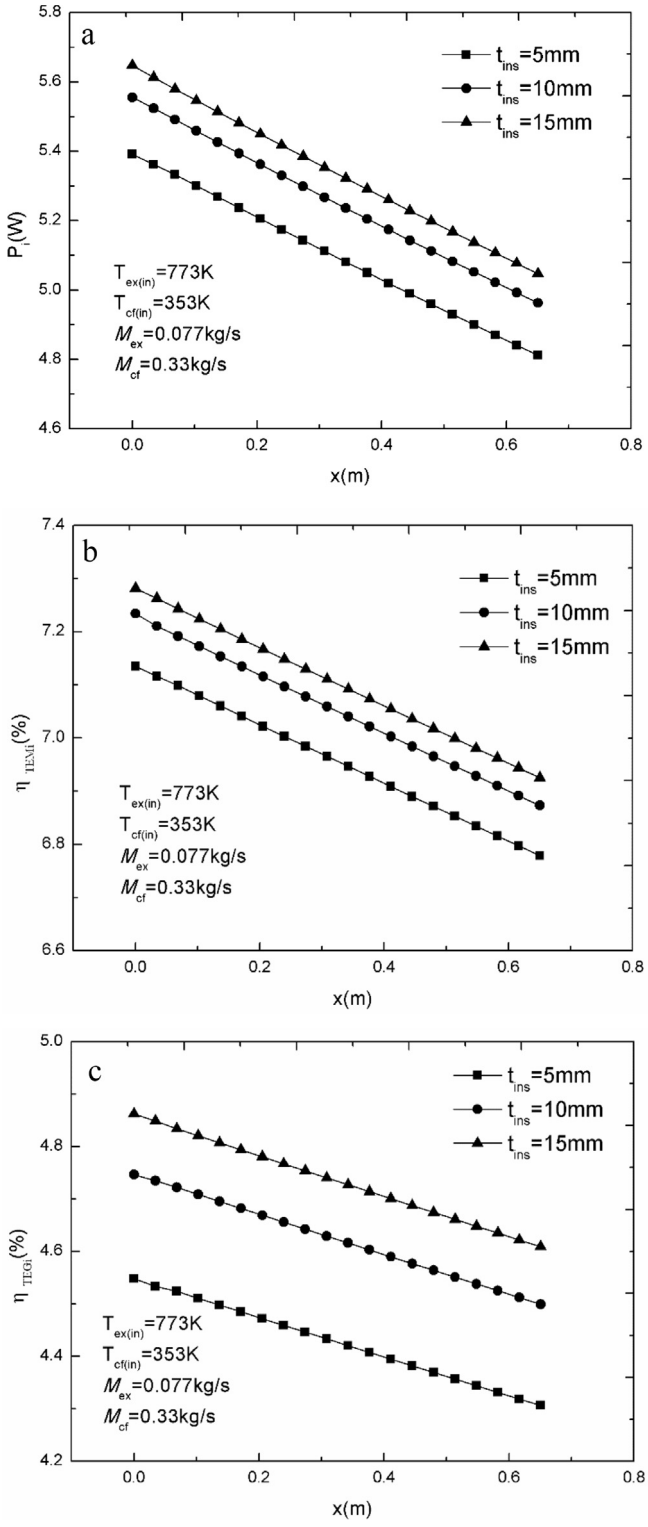


**Fig. 11.** a. Output power of each CV under different thicknesses of the insulation layer. b. TEM conversion efficiency of each CV under different thicknesses of the insulation layer. c. TEG conversion efficiency of each CV under different thicknesses of the insulation layer.

from the figures that the output performances of each CV drops linearly, which is consistent with the conclusion obtained from Fig. 10. The thicker the insulation layer is, the higher output power and conversion efficiencies are. It is because that the thermal resistance increases with the thickness of the insulation layer, so the heat conducted through the insulation layer becomes less, and the heat being taken away to the environment through air natural convection becomes less too. The total amount of the heat exchanged between the exhaust flow and the tube wall is the summation of the heat conducted to heat transfer fins and those being taken away through the air natural convection on the surface of the insulation layer, so increasing the thickness of the insulation layer helps to enhance heat conducting to the heat transfer fins, the output power and the conversion efficiencies can naturally be higher as well. The output power for the whole TEG model should be recognized as the $P_m$ in Eq. (29), the average insulation layer thickness contribution rate to the output power $CR_{\text{insulation layer thickness}}$ is 0.49 W/mm.

Fig. 12 shows the variations of output power, the TEM conversion efficiency and the TEG conversion efficiency for the whole TEG model with the inlet temperature of exhaust, the thickness of the insulation layer is 10 mm and $b$ is 15 mm. As it can be seen, with the increasing of the exhaust inlet temperature, more heat is carried to conduct through the exhaust tube wall, so the output performances improve as well. The average exhaust inlet temperature contribution rate to the output power $CR_{\text{exhaust inlet temperature}}$ is 0.52 W/K. In the engineering applications, TEG can be arranged on the front position of the exhaust tube as possible to get a higher exhaust temperature.

In addition to improve the exhaust inlet temperature, it can also reduce the coolant temperature to enhance the output performance of TEG, both of these methods mean to increase $\Delta T_{TE}$. Fig. 13 shows the variations of the output power, the TEM conversion efficiency and the TEG conversion efficiency for the whole TEG model with the inlet temperature of the coolant, the thickness of the insulation layer is 10 mm and $b$ is 15 mm. It is clear that as the coolant temperature decreases, the output power and the thermal conversion efficiencies have been significantly improved, the average coolant inlet temperature contribution rate to the output power $CR_{\text{coolant inlet temperature}}$ is −0.77 W/K ("−" means the output power increases when the coolant inlet temperature decreases, and vice versa), whose absolute value is higher than $CR_{\text{exhaust inlet temperature}}$.

Although reducing the inlet temperature of the coolant is significant to improve the output performance of TEG, since the TEG cooling cycle uses a branch of the engine cooling system, adding a separate cooling system or an intercooled equipment for the existing TEG will result in additional power consumption, and it needs to re-analyse the contribution of TEG to the fuel economy of vehicle.

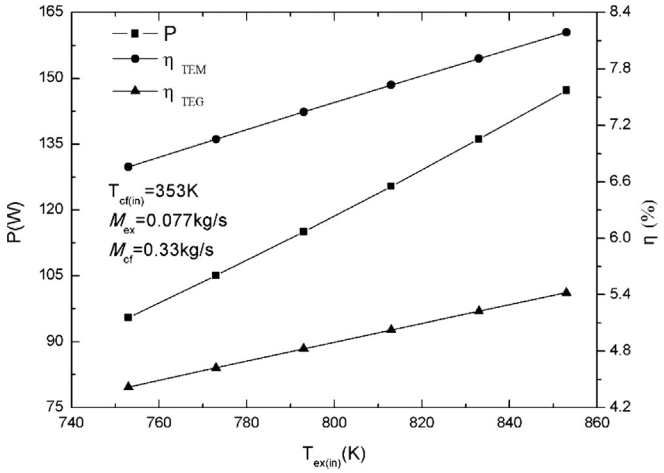


**Fig. 12.** Variations of the output power, the TEM conversion efficiency and the TEG conversion efficiency for the whole TEG model with the inlet temperature of exhaust.

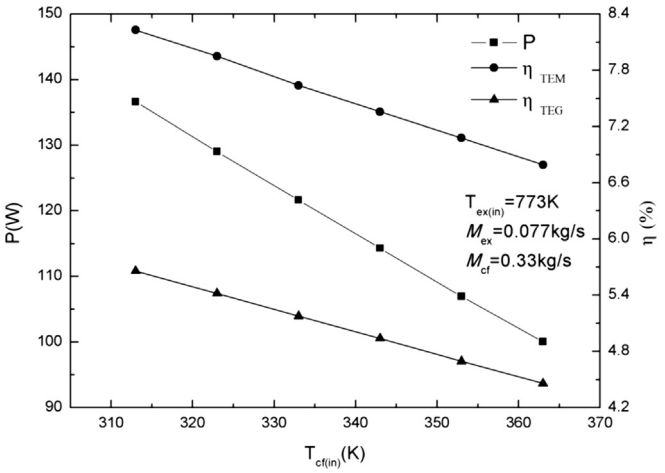


**Fig. 13.** Variations of the output power, the TEM conversion efficiency and the TEG conversion efficiency for the whole TEG model with the inlet temperature of coolant.

Fig. 14 shows the variations of the output power with the exhaust inlet mass flow rate under different exhaust inlet temperatures, the thickness of the insulation layer is 10 mm and $b$ is 15 mm. As the exhaust mass flow rate increases, the output power of TEG increases obviously. The higher the exhaust inlet temperature is, the faster the output power rises. The variations of the TEM and the TEG conversion efficiencies with the exhaust inlet mass flow rate under different exhaust inlet temperatures are shown in Fig. 15. Similar to Fig. 14, the TEM and the TEG conversion efficiencies increase with the increasing of the exhaust inlet mass flow rate. In Fig. 11, the average exhaust inlet mass flow contribution rate to the output power $CR_{\text{exhaust inlet mass flow rate}}$ is 985 W/(kg/s), 1076.1 W/(kg/s) and 1170.8 W/(kg/s) respectively corresponding to the exhaust inlet temperature of 773 K, 793 K and 813 K. It shows that improving the exhaust inlet mass flow rate can obviously increase the output power under higher exhaust inlet temperatures.

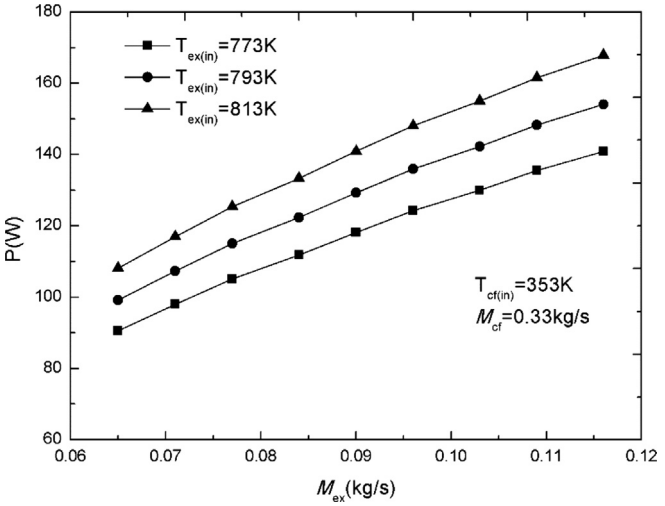


**Fig. 14.** Variations of the TEG output power with the exhaust inlet mass flow rate under different exhaust inlet temperatures.

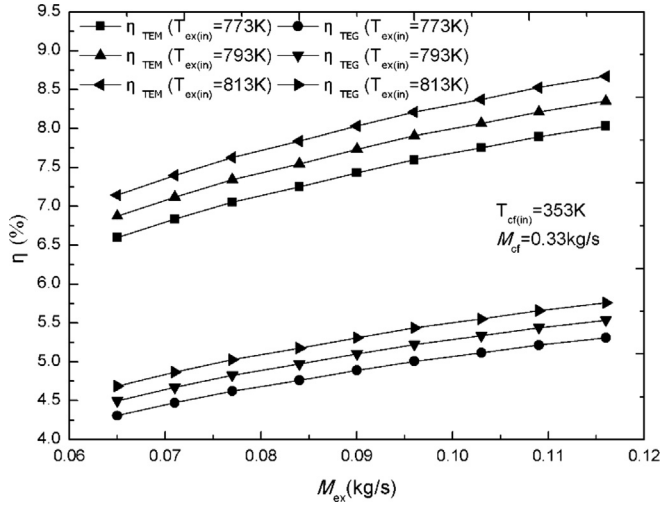


**Fig. 15.** Variations of the TEM and the TEG conversion efficiencies with the exhaust inlet mass flow rate under different exhaust inlet temperatures.

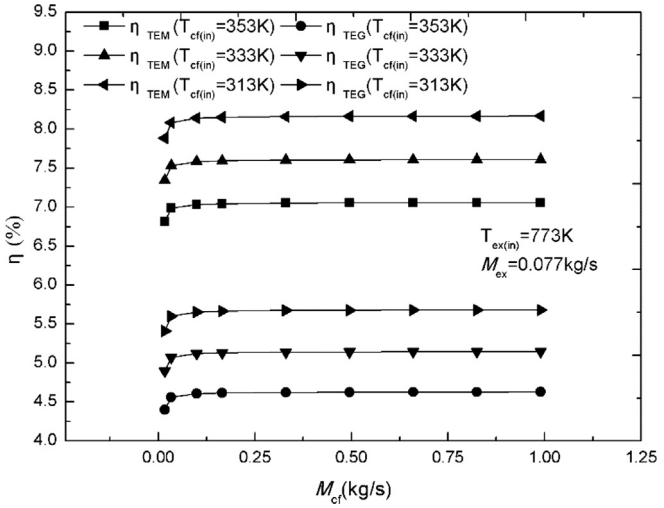


**Fig. 17.** Variations of the TEM and the TEG conversion efficiencies with the coolant inlet mass flow rate under different coolant inlet temperatures.

As is shown in Fig. 8, due to the relatively high specific heat capacity of the coolant, the temperature variation of coolant is less than 1 K. Fig. 16 shows the variations of the TEG output power with the coolant inlet mass flow rate under different coolant inlet temperatures, and Fig. 17 indicates the variations of the TEM and the TEG conversion efficiencies with the coolant inlet mass flow rate under different coolant inlet temperatures, the thickness of the insulation layer is 10 mm and $b$ is 15 mm for both of the two figures. As it can be seen, either for the output power, or the conversion efficiencies, the influence of the coolant inlet mass flow rate is very small after about 0.165 kg/s (the velocity of coolant is 0.5 m/s), which is due to the relatively high specific heat capacity of the coolant. Before this value, the output power and the conversion efficiencies change obviously with the increasing of the coolant inlet mass flow rate, which is called the "sensitive range". The average coolant inlet mass flow contribution rate to the output power $CR_{\text{coolant inlet mass flow rate}}$ in the sensitive range is 41.3 W/(kg/s), 46.9 W/(kg/s) and 52.8 W/(kg/s) respectively corresponding to the coolant inlet temperature of 353 K, 333 K and 313 K (certainly, since the density of exhaust and the density of coolant is not in an order of magnitude, this contribution rate should not be compared with $CR_{\text{exhaust inlet mass flow rate}}$).

Based on the above analyses, if maintaining the existing equipment and structure, increasing the exhaust inlet temperature and the mass flow rate, as well as lowering the coolant inlet temperature are useful methods to improve the output performance of TEG. The method of increasing the exhaust inlet temperature may be implemented by laying TEG on the front position of exhaust tube as possible, laying an insulation layer outside the shell of TEG, etc. All these methods will not generate any additional engine output power consumptions. Increasing the exhaust inlet mass flow rate and reducing the coolant inlet temperature both need to consume extra engine output power. The net output power of TEG $P_{\text{net}}$ should be equal to the output power generated by TEG minus the extra output power consumption, so the appropriate exhaust inlet mass flow rate and the coolant inlet temperature should be chosen in reason to maximize the $P_{\text{net}}$.

Fig. 18 shows the variations of the output power, the TEM conversion efficiency and the TEG conversion efficiency with $b$, which is the distance from the base of the heat transfer fin to TEM, the

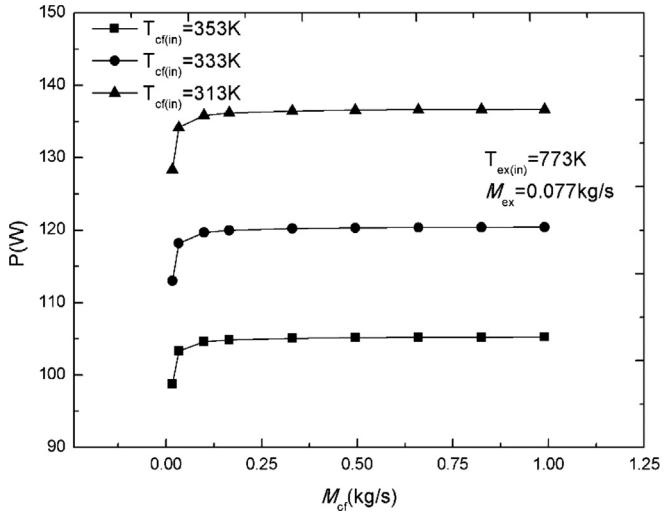


**Fig. 16.** Variations of the TEG output power with the coolant inlet mass flow rate under different coolant inlet temperatures.

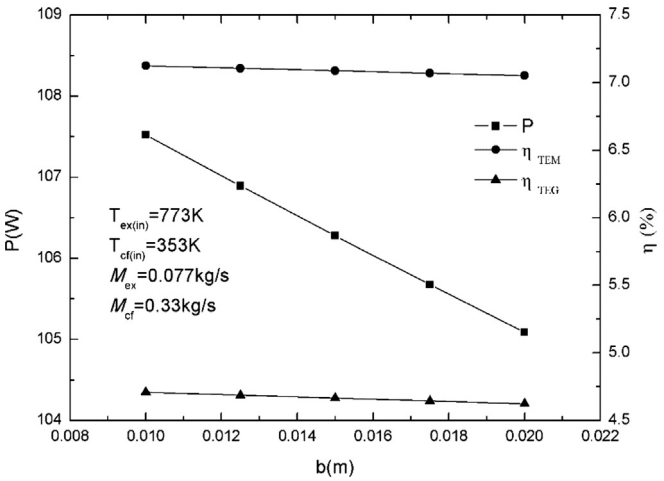


**Fig. 18.** Variations of the output power, the TEM conversion efficiency and the TEG conversion efficiency with $b$.

**Table 2**
Summary of the different $CR_{var}$.

| | | | |
|---|---|---|---|
| $CR_{insulation\ layer\ thickness}$ | 0.49 W/mm | | |
| $CR_{exhaust\ inlet\ temperature}$ | 0.52 W/K | | |
| $CR_{coolant\ inlet\ temperature}$ | −0.77 W/K | | |
| $CR_{exhaust\ inlet\ mass\ flow\ rate}$(773 K, 793 K, 813 K) | 985 W/(kg/s) | 1076.1 W/(kg/s) | 1170.8 W/(kg/s) |
| $CR_{coolant\ inlet\ mass\ flow\ rate}$(353 K, 333 K, 313 K before 0.165 kg/s) | 41.3 W/(kg/s) | 46.9 W/(kg/s) | 52.8 W/(kg/s) |
| $CR_b$ | −0.24 W/mm | | |

thickness of the insulation layer is 10 mm. The output power and the conversion efficiencies decrease to some extent with the increasing of $b$. Since the radial height of the fin in this numerical model is limited, the variation range of $b$ is only within a small interval. If the fin is higher, this effect will be more apparent. The average $b$ contribution rate to the output power $CR_b$ in this simulation is −0.24 W/mm. It can be concluded that in the case of an engineering perspective, TEM should be arranged in the position which is relatively close to the roots of the fin as possible to achieve better output performance.

Table 2 is the summary of different $CR_{var}$ obtained from the above analyses.

## 5. Conclusion

Based on the thermoelectric power generation theory, non-equilibrium thermodynamics theory, heat transfer theory and finite difference principle, a numerical model for TEG with cylindrical shell and straight fins is established. According to the different structures of exhaust tube, cylindrical shell and heat transfer fins, grids are divided separately in order to analyse the numerical model, and the contact effects are also taken into consideration. Along the axial direction, the temperatures of the exhaust and the coolant change linearly. Due to the relatively high specific heat capacity of the coolant, the temperature variation of the coolant is negligible. Laying an insulation layer outside the TEG cylindrical shell can effectively improve the output power of TEG. The influences of the inlet temperature and mass flow rate of the exhaust and the coolant are researched separately. By comparing the different variable contribution rates to the output power, it proves that increasing the inlet temperature and the inlet mass flow rate of the exhaust, as well as reducing the inlet temperature of the coolant are useful methods to improve the performance of TEG in a certain extent. However, some methods make additional power losses, and the input parameters need to be chosen appropriately to maximize the net output power of TEG. In addition, if conditions permit, TEM should be arranged near the root of heat transfer fin as possible.

The heat transfer numerical model established in this paper can not only be used for the newly designed TEG with cylindrical shell and straight fins, but also applied to the other types of TEG. The versatility of the numerical model can evaluate the output performance of TEG on the early stages of the designing process, and optimize the structural parameters, the external boundary conditions and the related input parameters.

The next step is to establish a more accurate model for TEG with cylindrical shell and straight fins in CFD simulation software environment, and make some research on the heat exchange process. Constructing and operating a scaled real TEG with cylindrical shell and straight fins, as well as testing the performance of the TEG to validate the reliability of the numerical model are also included in the program. By using the engine simulation software, the transient output data of exhaust can be obtained, so the real-time simulations of TEG will be carried out to evaluate its contribution to the fuel economy of vehicle.

## Nomenclature

| | |
|---|---|
| $A_{TEleg}$ | cross sectional area of thermocouple leg ($m^2$) |
| $a$ | side length of TEM (m) |
| $b$ | radial distance from the root of the heat transfer fin to TEM (m) |
| $C_p$ | constant-pressure specific heat (J/(kg K)) |
| CR | the average variable contribution rate to the output power |
| $d$ | diameter (m) |
| $Gr_{air}$ | Grashof number of air |
| $h$ | heat convection coefficient (W/($m^2$ K)) |
| $I$ | current (A) |
| $K$ | thermal conduction (W/m) |
| $L$ | total axial length of fin (m) |
| $L_{TEleg}$ | length of thermocouple leg (m) |
| $\dot{m}$ | mass flow rate (kg/s) |
| $N_{fin}$ | number of fins |
| $Nu_f$ | Nusselt number of fluid |
| $P$ | output power (W) |
| $Pr_f$ | Prandtl number of fluid |
| $Q_h$ | absorbing heat of TEM (W) |
| $Q_c$ | releasing heat of TEM (W) |
| $\dot{q}$ | heat mass flow (W) |
| $R$ | internal resistance of thermocouple (Ω) |
| $R_L$ | load resistance (Ω) |
| $R_{copper}$ | resistance of copper stripe (Ω) |
| $Re_f$ | Reynolds number of fluid |
| $T$ | absolute temperature (K) |
| $t$ | thickness (m) |
| $\alpha$ | Seebeck coefficient (V/K) |
| $\lambda$ | thermal conductivity (W/(m K)) |
| $\rho$ | density (kg/$m^3$) |
| $\nu_{air}$ | kinematic viscosity of air ($m^2$/s) |
| $\eta$ | heat conversion efficiency (W) |
| $\sigma$ | electrical resistivity (Ω m) |
| $\Delta x$ | axial length of the control volume (m) |
| $\Delta y$ | radial length of the control volume on fins (m) |

*Subscripts*

| | |
|---|---|
| cf | cooling fluid |
| cf-wall | between the cooling fluid and the tube wall |
| con_ex | convection of the exhaust |
| con_cf | convection of the cooling fluid |
| ct | cooling tube |
| cw | cooling tube wall |
| cyl | cylinder shell |
| ex | exhaust |
| ex_tube | exhaust tube |
| ex-wall | between the exhaust and the tube wall |
| fin_air | between the fin and air |
| $i$ | number of axial control volume |
| ins | insulation layer |
| $k$ | number of radial control volume for $i$th CV |
| surf | surface |
| tc | cold side of TEM |
| th | hot side of TEM |
| tw | tube wall |
| var | variable |

## References


[1] J.L. Yu, H. Zhao, A numerical model for thermoelectric generator with the parallel-plate heat exchanger, J. Power Sources 172 (2007) 428–434.
[2] K. Ono, R.O. Suzuki, Thermoelectric power generation: converting low-grade heat into electricity, J. Miner. Met. Mater. Soc. 50 (5) (1998) 12–31.
[3] R. Stobart, D. Milner, The potential for thermo-electric regeneration of energy in vehicles, SAE Tech. Pap. (2009), 2009-01-1333.
[4] M.V. Vedernikov, E.K. Jordanishvili, A.F. Ioffe and Origin of Modern Semiconductor Thermoelectric Energy Conversion, Proceedings of the 17th International Conference on Thermoelectrics, 1998.
[5] J. Esarte, G. Min, D.M. Rowe, Modelling heat exchangers for thermoelectric generators, J. Power Sources 93 (2001) 72–76.
[6] R.O. Suzuki, D. Tanaka, Mathematical simulation of thermoelectric power generation with the multi-panels, J. Power Sources 122 (2003) 201–209.
[7] R.O. Suzuki, D. Tanaka, Mathematic simulation on thermoelectric power generation with cylindrical multi-tubes, J. Power Sources 124 (2003) 293–298.
[8] F.K. Meng, L.G. Chen, F.R. Sun, A numerical model and comparative investigation of a thermoelectric generator with multi-irreversibilities, Energy 36 (2011) 3513–3522.
[9] D.T. Crane, G.S. Jackson, Optimization of cross flow heat exchangers for thermoelectric waste heat recovery, Energy Convers. Manag. 45 (2004) 1565–1582.
[10] Y.C. Wang, C.S. Dai, S.X. Wang, Theoretical analysis of a thermoelectric generator using exhaust gas of vehicles as heat source, Appl. Energy 112 (2013) 1171–1180.
[11] Y.Y. Hsiao, W.C. Chang, S.L. Chen, A mathematic model of thermoelectric module with applications on waste heat recovery from automobile engine, Energy 35 (2010) 1447–1454.
[12] J.H. Yang, Development of Thermoelectric Technology for Automotive Waste Heat Recovery, FY2008 DOE Vehicle Technologies Annual Merit Review, 2008.
[13] A. Eder, Thermoelectric Power Generation – the Next Step to Future $CO_2$ Reductions, Presentation to DEER conference, 2009.
[14] W.Q. Tao, Numerical Heat Transfer, Xi'an Jiaotong University Press, 2001, pp. 28–29 (in Chinese).
[15] Y.Z. Cao, Heat Transfer, Beihang University Press, 2001, pp. 124–130 (in Chinese).
[16] R.G. Wu, X. Li, Y.H. Zhang, et al., Preparation and thermoelectric properties of hot-pressed PbTe-based alloys, J. Mater. Sci. Eng. 124 (2010) 271–274.
[17] M. Gao, D.M. Rowe, Thermoelectric and Its Applications, Weapon Industry Press, 1996, pp. 12–19 (in Chinese).